


## FULL PAPER

# Click chemistry based regioselective one-pot synthesis of coumarin-3-yl-methyl-1,2,3-triazolyl-1,2,4-triazol-3(4H)-ones as newer potent antitubercular agents

Shilpa M. Somagond<sup>1</sup> | Ravindra R. Kamble<sup>1</sup>  | Praveen K. Bayannavar<sup>1</sup> |  
Saba Kauser J. Shaikh<sup>1</sup> | Shrinivas D. Joshi<sup>2</sup> | Vijay M. Kumbar<sup>3</sup> | Aravind R. Nesaragi<sup>1</sup> |  
Mahadevappa Y. Kariduraganavar<sup>1</sup>

<sup>1</sup>Department of Studies in Chemistry, Karnatak University Dharwad, Karnataka, India

<sup>2</sup>Novel Drug Design and Discovery Laboratory, Department of Pharmaceutical Chemistry, S.E.T.'s College of Pharmacy, Dharwad, Karnataka, India

<sup>3</sup>Dr. Prabhakar Kore Basic Science Research Center, KLE University, Belagavi, Karnataka, India

## Correspondence

Dr. Ravindra R. Kamble, Department of Studies in Chemistry, Karnatak University Dharwad, Karnataka 580003, India.  
Email: kamchem9@gmail.com

## Funding information

University Grants Commission (UGC) "Antitumor activity an integrated Approach" a focused area of UPE FAR-I programme, Grant/Award Number: F. No. 14-3/2012 (NS/PE) Dated: 14-03-2012

## Abstract

Coumarin-3-yl-methyl-1,2,3-triazolyl-1,2,4-triazol-3(4H)-ones (**8k–z**) were synthesized *via* copper(I)-catalyzed azide–alkyne cycloaddition click chemistry. The synthesized hybrid molecules were characterized by spectral studies. Compounds **8k–z** were screened for their *in vitro* anti-TB activity by using the Microplate Alamar Blue assay and for cytotoxicity using the MTT assay. Some of the compounds were found to be most potent against the tested *Mycobacterium tuberculosis* H37Rv strain with a MIC of 1.60 µg/ml. Further, docking the compounds into the InhA binding pocket showed strong binding interactions and effective overall docking scores were recorded. The drug-likeness and toxicity studies were computed using Molinspiration and Protox, respectively.

## KEYWORDS

2H-chromen-2-one, antitubercular activity, click reaction, cytotoxicity, drug likeness, molecular docking, toxicity prediction

## 1 | INTRODUCTION

Tuberculosis (TB) is a lung disease generally caused by *Mycobacterium tuberculosis* (Mtb), which leads to the death of almost 3 million people every year and it is found to be a prominent bacterial infectious agent.<sup>[1,2]</sup> The rising drug resistance and poor activity of accessible therapies towards the concealed stage of Mtb infection have created a clear need to develop new medicine to treat TB.<sup>[3]</sup> Thus, fast-acting medicines with different mechanisms of action that are not cross defiant to the existing drugs are being keenly preferred. To overcome this drawback two initial screening methods were being applied in TB drug discovery-target. First, high throughput screening and makeup minimum inhibitory concentration (MIC) based on the screening of entire cell bacteria. Second, the enzyme-based high throughput screening for novel TB drugs has been generally adopted; this methodology has not formed

prominent successes. Therefore, to understand these mirrors of success that proceed towards in other antibacterial drug discovery programs<sup>[4]</sup>

Presently, there is an overwhelming call to develop new structural categories of antitubercular agents that permit shorter and additional effective therapies. Triazoles are shown to possess a variety of fascinating features within the framework of medicinal chemistry. They are stable to acidic/basic reaction and conjointly reductive/oxidative conditions, investigative of a high aromatic stabilization and this scaffold is comparatively resistant to metabolic degradation. The best-known examples of triazole containing structure are tazobactam, a β-lactamase inhibitor with the broad-spectrum antibiotic piperacillin.<sup>[5–7]</sup> And also several 1,2,3-triazole analogs **1–5** (Figure 1)<sup>[8–11]</sup> have been reported with antitubercular activity. In addition, 1,2,3-triazoles are found in herbicides, fungicides, and dyes.<sup>[12]</sup>

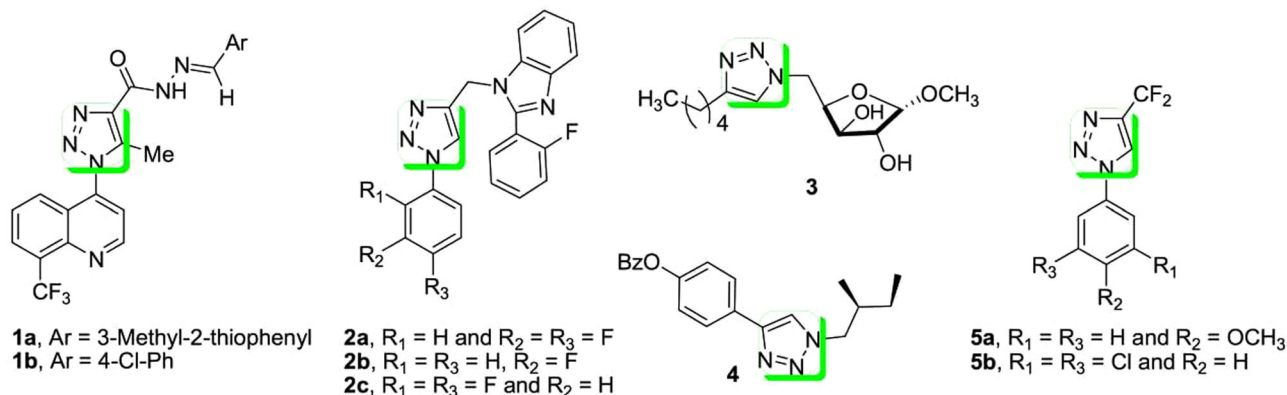


**FIGURE 1** Tuberculostatic 1,2,3-triazoles 1–5

1,2,3-Triazoles have been of interest to medicinal chemists as Sharpless initially introduced the concept of click chemistry, by that the Huisgen's [2+3] cycloaddition reaction of organic azides and terminal alkynes will be efficiently catalyzed by copper(I) ions and may be performed at ambient temperature, which results in the formation of single product viz., 1,4-regioisomer of 1,2,3-triazole.<sup>[13–16]</sup> Copper(I) catalyzed chemical action of this transformation accelerates the speed of reaction up to 10<sup>7</sup> times and hence has placed it in a class of its own and has facilitated many novel applications.<sup>[17–22]</sup>

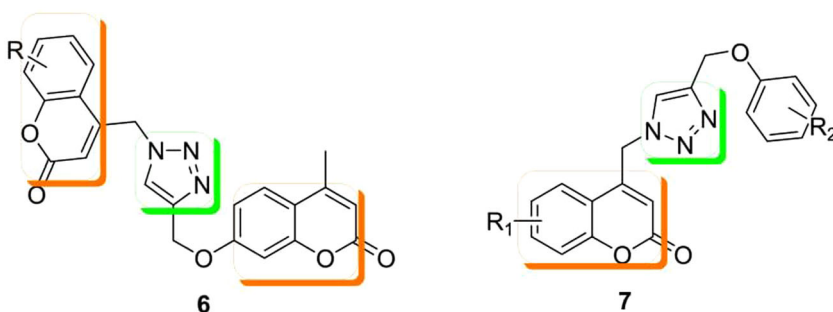
Coumarin (2H-chromen-2-one), an oxygen heterocycle present in the plants, which consists of various phenolic substances and is composed of combined benzene and 2-pyrone ring systems. Thirteen hundred coumarins are distinctive as secondary metabolites from plants, microorganisms, and fungi.<sup>[23,24]</sup> Coumarin and its derivatives have diverse pharmacological activities such as antibacterial,<sup>[25]</sup> antifungal,<sup>[26]</sup> anticoagulant,<sup>[27]</sup> antihypertensive,<sup>[28]</sup> anti-HIV,<sup>[29,30]</sup> antioxidant,<sup>[31]</sup> scavenging reactive oxygen species,<sup>[32]</sup> antituberculosis,<sup>[33]</sup> anticonvulsant,<sup>[34]</sup> antihyperglycemic,<sup>[35]</sup> anticancer,<sup>[36]</sup> and anti-inflammatory.<sup>[37]</sup> Thus, the synthesis of coumarin and its analogs has established growing attention to synthetic organic chemists as well as biologists. 1,4-Disubstituted bis-chromenyl 1,2,3-triazole hybrids **6** and mono-chromenyl 1,2,3-triazole hybrids **7** (Figure 2) have been synthesized and studied *in vitro* for anti-TB activities against *M. tuberculosis* H37Rv (*M.tb*).<sup>[38]</sup>

1,2,4-Triazole derivatives have received great attention during the past two decades as prospective antimicrobial agents.<sup>[39]</sup> Also, most of the existing antifungal drugs hold 1,2,4-triazole

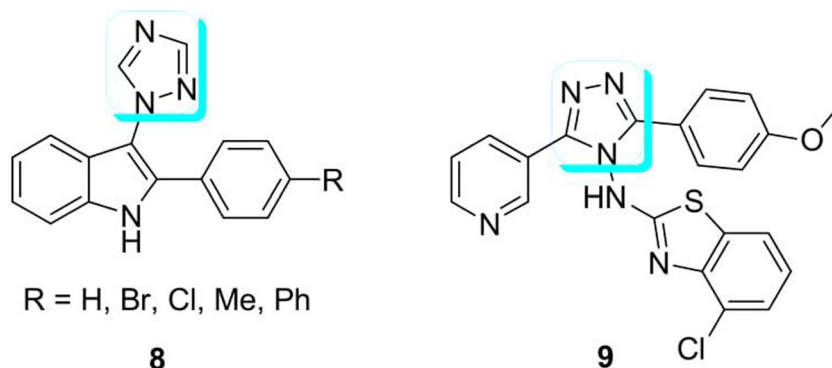
pharmacophore in their elemental structures which proves the antifungal potencies of the 1,2,4-triazole template so that it expresses significant antimicrobial activity.<sup>[40]</sup> Several 1,2,4-triazole derivatives have been screened for incising novel promising anti-TB candidates. Some 1,2,4-triazole appended indole hybrids **8**<sup>[41]</sup> with substituted phenyl ring at 2<sup>nd</sup> position of indole and 1,2,4-triazole derivatized benzothiazole **9**<sup>[42]</sup> have exhibited anti-TB activity against MTB H37Rv (Figure 3; MIC: 0.5 mg/ml). Hence, we were also prompted to work on the preparation of 1,2,4-triazole using *N*-arylsydnone which belongs to mesoionic class of compounds. *N*-Arylsydnone act as functional and novel precursor for the synthesis of various biologically active heterocycles viz., pyrazoles, 1,3,4-oxadiazoles, phenyl indazoles, pyrazolines, and tetrazines via 1,3-dipolar cycloaddition and addition elimination reactions.<sup>[43]</sup>

In addition, to explore the mechanism of action of title compounds **8k–z** and provide guidance for new drug design, SAR analysis (Figure 4) of the reported molecules was carried out which revealed the following information.

- 1,2,4-Triazole nucleus displayed promising anti-TB potency against drug-sensitive and DR-TB including MDR-TB, warrant further appraisal as a novel agent to control TB in humans.<sup>[44,45]</sup> The aromatic substitutions are preferred; the substitution at the 4th position of the aromatic substituent follow the trend –OCH<sub>3</sub> > –H.
- 1,2,3-Triazole as a linker to combine different anti-TB active skeleton<sup>[46]</sup> suggesting that the presence of 1,2,3-triazole moiety extremely improves the efficiency.



**FIGURE 2** Chemical structures of coumarin 1,2,3-triazole hybrids as anti-TB agents

**FIGURE 3** 1,2,4-Triazole nucleus containing potent antitubercular agents

(iii) It is evident from the SAR study that the bioactive skeleton having the aforementioned substitution at positions 6 and 7 and halogen (Br, Cl) at C-6 position of the coumarin core found responsible for the potent activity compared to methoxy, methyl, benzo-substitutions (Figure 4).<sup>[47]</sup>

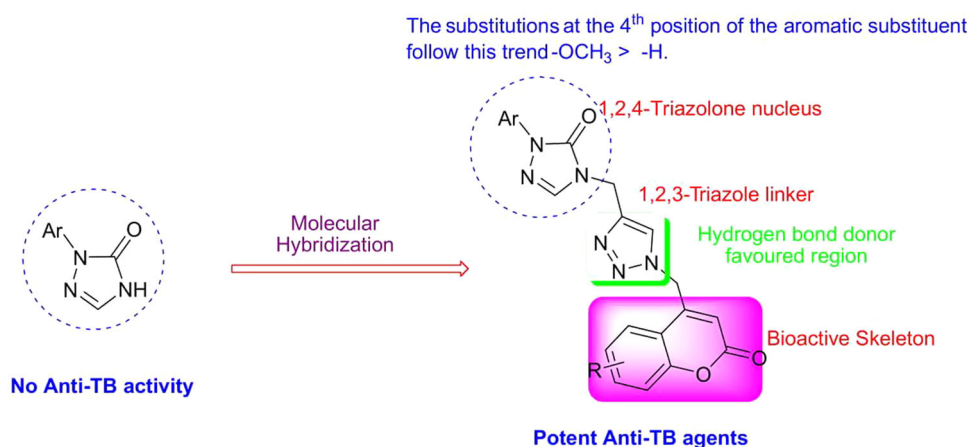
Moreover, a recent inclination in medicinal chemistry illustrates the recognition of molecular hybridization for drug design and development. This has supported combining pharmacophoric units of various bioactive substances to form a new hybrid molecule with increased effects evaluated in comparison to the parent drug.<sup>[48-50]</sup> Thus, in the present study new hybrid molecules are reported which are formed by the combination of three different pharmacophoric units such as coumarin, 1,2,3-triazole, and 1,2,4-triazole. Further a library of coumarin-3-yl-methyl-1,2,3-triazolyl-1,2,4-triazol-3(4H)-ones **8k-z** hybrids were synthesized by click chemistry approach. The structures of these hybrid molecules were characterized by FT-IR, <sup>1</sup>H NMR, <sup>13</sup>C NMR, mass spectral data and elemental analysis. *In vitro* antitubercular activity of title compounds have been carried out against pathogenic strain *M. tuberculosis* H37Rv strain and also carried out the cytotoxicity evaluation. The computational study (molecular docking) revealed the competent interaction of hybrid molecules with inhibition of enzyme InhA-D148G which assisted in parallel to *in vitro* anti-TB activity. Moreover, *in silico* pharmacokinetic

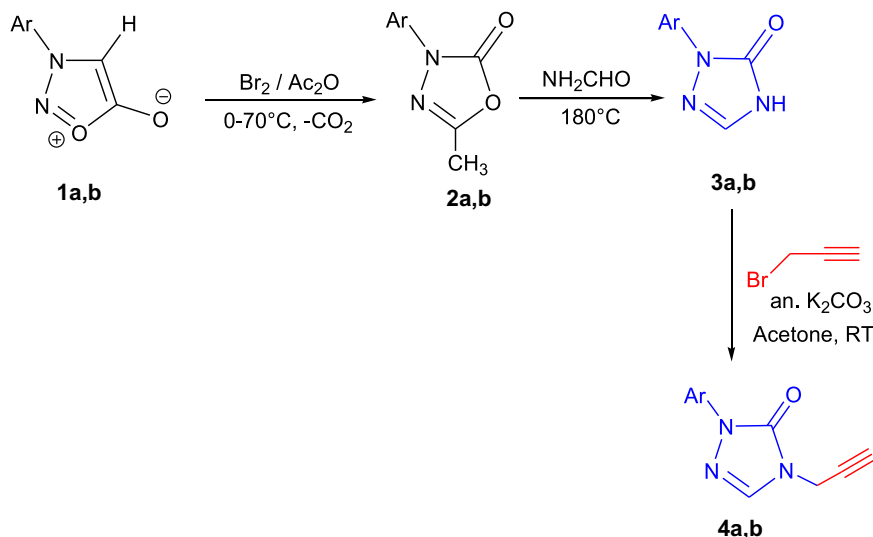
and toxicity studies were carried out computationally to get an insight into the structural parameters leading to biological activity.

## 2 | RESULTS AND DISCUSSION

### 2.1 | Synthesis

Acetylenic dipolarophile **4a,b** was prepared by the reaction of substituted 2-aryl-2H-1,2,4-triazol-3(4H)-one **3a,b** with 3-bromoprop-1-yne employing potassium carbonate in anhydrous acetone (Scheme 1). The ethyl-4-bromoacetoacetate was synthesized from bromination of ethylacetoacetate in dry ether at 0–5°C. Under Pechmann cyclisation, it was reacted with various substituted phenols in presence of conc. sulfuric acid as cyclising agent.<sup>[50]</sup> This reaction ends up with the formation of required synthon 4-bromomethyl coumarin **6c-j** (Scheme 2). The corresponding dipolar azide **7c-j** was obtained by treating **6c-j** with sodium azide (NaN<sub>3</sub>) in aqueous acetone at room temperature. This was followed by azide-alkyne cycloaddition of the acetylenic dipolarophiles **4a,b** and 4-azidomethyl coumarins **7c-j** in presence of copper ascorbate (generated *in situ*) in THF/water, 1:1 at room temperature to get exclusively one product, that is, coumarinyl-1,2,3-triazolyl-1,2,4-triazol-3(4H)-ones **8k-z** in excellent yields and purity (Scheme 2).

**FIGURE 4** Rational molecular hybridization design

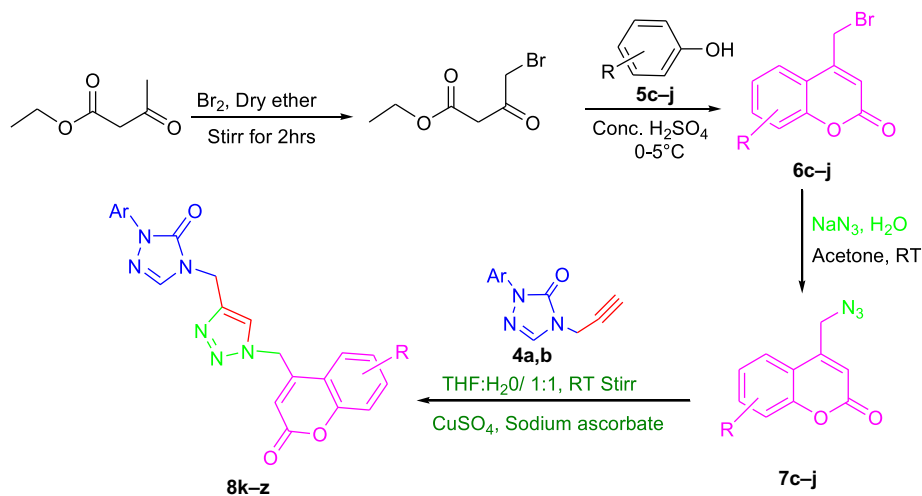
**SCHEME 1** Synthesis of acetylenic dipolarophile **4a,b**

**a:** Ar = C<sub>6</sub>H<sub>5</sub>; **b:** Ar = 6-OCH<sub>3</sub>-C<sub>6</sub>H<sub>4</sub>

## 2.2 | Spectral characterization

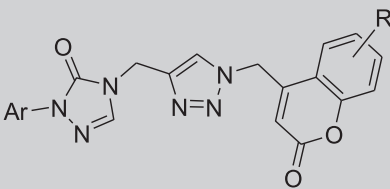
Formation of coumarinyl-1,2,3-triazolyl-1,2,4-triazol-3(4H)-ones **8k-z** is supported by spectroscopic studies viz., FT-IR, <sup>1</sup>H NMR, <sup>13</sup>C NMR and MS. FT-IR spectral analysis of compounds **8k-z** showed a sharp band in the range 1,710–1,730 cm<sup>-1</sup> due to the carbonyl stretching of coumarin moiety. Another sharp band in the range 1,690–1,715 cm<sup>-1</sup> and a medium intense band in the range 1,640–1,610 cm<sup>-1</sup>, respectively correspond to the C=O and C=N stretching of 1,2,4-triazolin-3-one ring. <sup>1</sup>H NMR spectral analysis showed two singlets

for CH<sub>2</sub> protons attached to 1,2,4-triazolin ring and coumarin moiety at 5.00–5.99 ppm and 4.93–5.08 ppm, respectively. The C<sub>5</sub>-H of 1,2,3-triazolin and C<sub>5</sub>-H of 1,2,4-triazolin ring appeared as a singlet in the range 7.70–8.46 ppm and 7.78–8.51 ppm, respectively. The C<sub>3</sub>-H of coumarin resonated as a singlet in the range 5.95–6.49 ppm. <sup>13</sup>C NMR spectral analyses showed the number of signals equivalent to the magnetically non-equivalent carbon atoms. Also, the mass spectral analyses showed the molecular ion peak corresponding to the molecular mass of title compounds.



**c:** R = 6-CH<sub>3</sub>; **d:** R = 6-Cl; **e:** R = 6-OCH<sub>3</sub>; **f:** R = 7-CH<sub>3</sub>; **g:** R = 5,7 Di-CH<sub>3</sub>; **h:** R = benzo[f]; **i:** R = benzo[h]; **j:** R = 4-tert-butyl; **k:** Ar = C<sub>6</sub>H<sub>5</sub>, R = 6-CH<sub>3</sub>; **l:** Ar = C<sub>6</sub>H<sub>5</sub>, R = 6-Cl; **m:** Ar = C<sub>6</sub>H<sub>5</sub>, R = 6-OCH<sub>3</sub>; **n:** Ar = C<sub>6</sub>H<sub>5</sub>, R = 7-CH<sub>3</sub>; **o:** Ar = C<sub>6</sub>H<sub>5</sub>, R = 5,7 Di-CH<sub>3</sub>; **p:** Ar = C<sub>6</sub>H<sub>5</sub>, R = benzo[f]; **q:** Ar = C<sub>6</sub>H<sub>5</sub>, R = benzo[h]; **r:** Ar = C<sub>6</sub>H<sub>5</sub>, R = 4-tert-butyl; **s:** 4-OCH<sub>3</sub>-C<sub>6</sub>H<sub>4</sub>, R = 6-CH<sub>3</sub>; **t:** 4-OCH<sub>3</sub>-C<sub>6</sub>H<sub>4</sub>, R = 6-Cl; **u:** 4-OCH<sub>3</sub>-C<sub>6</sub>H<sub>4</sub>, R = 6-OCH<sub>3</sub>; **v:** 4-OCH<sub>3</sub>-C<sub>6</sub>H<sub>4</sub>, R = 7-CH<sub>3</sub>; **w:** 4-OCH<sub>3</sub>-C<sub>6</sub>H<sub>4</sub>, R = 5,7-di-CH<sub>3</sub>; **x:** 4-OCH<sub>3</sub>-C<sub>6</sub>H<sub>4</sub>, R = benzo[f]; **y:** 4-OCH<sub>3</sub>-C<sub>6</sub>H<sub>4</sub>, R = benzo[h]; **z:** 4-OCH<sub>3</sub>-C<sub>6</sub>H<sub>4</sub>, R = 4-tert-butyl

**SCHEME 2** Schematic representation for the synthesis of coumarinyl-1,2,3-triazolyl-1,2,4-triazol-3(4H)-on **8k-z**

**TABLE 1** In vitro antitubercular evaluation of MIC ( $\mu\text{g/ml}$ ) of title compounds **8k–z**


Entry	Ar	R	MIC ( $\mu\text{g/ml}$ )	IC <sub>50</sub> ( $\mu\text{g/ml}$ )	SI
<b>8k</b>	Phenyl	6-CH <sub>3</sub>	3.12	477.40	153.01
<b>8l</b>	Phenyl	6-Cl	6.25	291.20	046.59
<b>8m</b>	Phenyl	6-OCH <sub>3</sub>	3.12	127.60	040.90
<b>8n</b>	Phenyl	6-t-Butyl	3.12	111.10	035.61
<b>8o</b>	Phenyl	7-CH <sub>3</sub>	1.60	769.30	480.81
<b>8p</b>	Phenyl	5,6-Benzo	1.60	072.13	045.08
<b>8q</b>	Phenyl	7,8-Benzo	6.25	228.10	036.50
<b>8r</b>	Phenyl	5,7-Di-CH <sub>3</sub>	12.5	292.80	023.42
<b>8s</b>	<i>p</i> -Anisyl	6-CH <sub>3</sub>	1.60	1087.00	679.38
<b>8t</b>	<i>p</i> -Anisyl	6-Cl	1.60	1438.00	898.75
<b>8u</b>	<i>p</i> -Anisyl	6-OCH <sub>3</sub>	3.12	125.20	040.13
<b>8v</b>	<i>p</i> -Anisyl	6-t-Butyl	1.60	017.81	011.13
<b>8w</b>	<i>p</i> -Anisyl	7-CH <sub>3</sub>	1.60	114.70	071.69
<b>8x</b>	<i>p</i> -Anisyl	5,6-Benzo	1.60	078.54	049.09
<b>8y</b>	<i>p</i> -Anisyl	7,8-Benzo	6.25	053.21	008.51
<b>8z</b>	<i>p</i> -Anisyl	5,7-Di-CH <sub>3</sub>	12.5	493.00	039.44
Std	-	-	3.12	ND	ND

Note: Std, pyrazinamide.

Abbreviation: MIC, minimum inhibitory concentration.

## 2.3 | Pharmacological evaluation

### 2.3.1 | In vitro antitubercular activity

In view of the intermolecular interactions and hydrogen binding modes of newly synthesized coumarinyl-1,2,3-triazolyl-1,2,4-triazol-3(4*H*)-ones **8k–z** with InhA-D148G mutant in complex with NADH (PDB: 4DQU) by docking simulation, the in vitro antitubercular activity was evaluated against *M. tuberculosis* H37Rv strain in eight different concentrations by using a Microplate Alamar Blue assay (MABA) method with pyrazinamide as standard. Results for the tested compounds are tabulated in Table 1, as MIC and the activity ranged from 12.5 to 1.6  $\mu\text{g/ml}$ . The MIC of the tested compounds were compared with standard drugs which indicated that almost all the newly synthesized compounds showed lower MIC values with potent inhibitory activity against *M. tuberculosis* H37Rv strain.

The antitubercular activity revealed that compounds **8o** (*methyl* at C<sub>7</sub> position of the coumarin), **8p** (*benzo* at C<sub>5</sub> and C<sub>6</sub> position of the coumarin), **8s** (*methyl* at C<sub>6</sub> position of the coumarin, *p*-methoxyphenyl at C<sub>1</sub> position of the 1,2,4-triazole), **8t** (*chloro* at C<sub>6</sub> position of the coumarin, *p*-methoxy phenyl substitution at C<sub>1</sub> position of the 1,2,4-triazole), **8v** (*t-butyl* at C<sub>6</sub> position of the

coumarin, *p*-methoxy substitution at C<sub>1</sub> position of the 1,2,4-triazole), **8w** (*methyl* at C<sub>7</sub> position of the coumarin, *p*-methoxy at C<sub>1</sub> position of the 1,2,4-triazole), **8x** (*benzo* at C<sub>5</sub> and C<sub>6</sub> position of the coumarin, *p*-methoxy phenyl at C<sub>1</sub> position of the 1,2,4-triazole) showed excellent activity having MIC as low as 1.6  $\mu\text{g/ml}$  which proved better than the standard drug pyrazinamide having MIC of 3.12  $\mu\text{g/ml}$  against *M. tuberculosis* H37Rv. Compounds **8k** (*methyl* at C<sub>7</sub> position of the coumarin), **8m** (*methoxy* at C<sub>7</sub> position of the coumarin), **8n** (*t-butyl* at C<sub>7</sub> position of the coumarin), **8u** (*methoxy* at C<sub>6</sub> position of the coumarin, *p*-methoxy phenyl at C<sub>1</sub> position of the 1,2,4-triazole) were more active as that of pyrazinamide with MIC of 3.12  $\mu\text{g/ml}$ . Compounds **8l**, **8r**, **8q**, **8y**, and **8z** showed good to moderate activity with MIC of 6.25–12.5  $\mu\text{g/ml}$ .

The electron-donating groups on coumarin and the phenyl ring attached to 1,2,4-triazole were generally observed to enhance the antitubercular activity (*viz.*, **8o**, **8p**, **8s**, **8t**, **8v**, **8w**, and **8x**) with MIC 1.6  $\mu\text{g/ml}$ . It is well known from the literature that the existence of these groups imparts a variety of properties including metabolic stability, steric, electronic properties, enhanced binding interactions, changes in physical properties and selective reactivities.<sup>[51]</sup>

The cytotoxicity results (Table 1), expressed as the IC<sub>50</sub> for the HEK293 (human embryonic kidney) cell line explain that all of the tested compounds **8k–z** showed very low cytotoxicity (IC<sub>50</sub> value ranging from 53.21 to 898.75  $\mu\text{g/ml}$ ). Pavan et al. reported that isoniazid and rifampicin, first-line drugs in current TB treatment, had IC<sub>50</sub> values of 1250 and 156.3  $\mu\text{g/ml}$ , respectively.<sup>[52]</sup> The selectivity index (SI) of each compound was calculated by dividing IC<sub>50</sub> by the MIC (Table 1). According to Orme et al.<sup>[53]</sup> candidates for new drugs must have a selective index equal or higher than 10, with MIC lower than 6.25  $\mu\text{g/ml}$  and low cytotoxicity. SI is used to estimate the therapeutic window of a drug and to identify drug candidates for further studies. Thus, in this study, it has been identified that compounds **8k**, **8o**, and **8s**, with SI values of 153.01, 480.81, and 679.38, respectively as very promising new TB drug candidates. The SI of compound **8t**, for example, was 898.75 and this index is comparable to the SI of rifampicin (MIC = 0.2  $\mu\text{g/ml}$ , IC<sub>50</sub> = 156.3  $\mu\text{g/ml}$ : SI = 781<sup>[54]</sup>), which is used together with isoniazid to treat TB.

### 2.3.2 | Molecular docking studies

To investigate the detailed intermolecular interactions between the ligand and the target protein, Surflex-Dock program was used. Docking studies give a fair idea related to drug–receptor interactions. Three-dimensional structure information on the target protein was taken from the PDB entry 4DQU. The processing of the protein integrated the removal of the ligand and the solvent molecules as well as the addition of hydrogen atoms. All the 16 inhibitors were docked into the active site of enzyme as shown in Figure 5 to compare with the in vitro antitubercular studies. The predicted binding energies of the compounds are listed in Table 2.

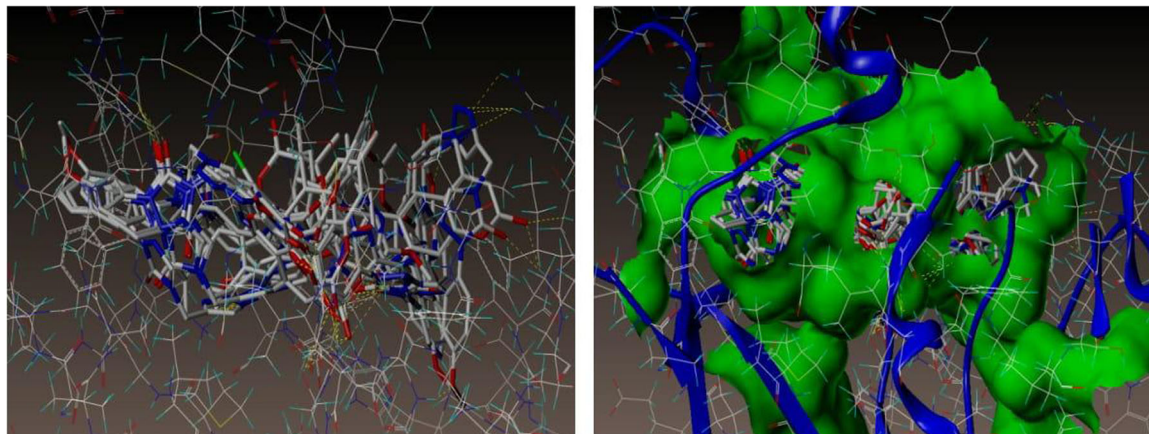


**FIGURE 5** Docked view of all the title compounds at the active site of the enzyme InhA-D148G

As depicted in Figure 6, the compound **8x** makes four hydrogen-bonding interactions at the active site of the enzyme InhA-D148G (PDB ID: 4DQU), among them two bonding interactions were raised from 1st nitrogen atom of triazole ring with hydrogens of ARG43 ( $-N-H-ARG43$ , 2.18 & 2.36 Å), 2nd nitrogen atom of 1,2,3-triazole ring makes a bonding interaction with hydrogen of ARG43 ( $-N-H-ARG43$ , 2.83 Å), oxygen atom of carbonyl group present on the 1,2,4-triazole ring makes a bonding interaction with hydrogen of ASP42 ( $-C=O-H-ASP42$ , 2.32 Å) and remaining one interaction came from

the oxygen atom of methoxy group present on the phenyl ring attached to 1,2,4-triazole with hydrogen atom of GLY14 ( $-O-H-GLY14$ , 1.80 Å) amino acid.

As depicted in Figure 7, the compound **8t** makes six hydrogen bonding interactions at the active site of the enzyme InhA-D148G (PDB ID: 4DQU), among them one bonding interaction was raised from 1st nitrogen atom of 1,2,3-triazole ring with hydrogen of GLY96 ( $-N-H-GLY96$ , 2.30 Å), 3rd nitrogen atom of 1,2,4-triazole ring makes a bonding interaction with hydrogen of SER20 ( $-N-H-SER20$ ,

**TABLE 2** Surflex docking score (kcal/mol) of the title compounds **8k–z** on enzyme InhA-D148G (PDB ID: 4DQU)

Code	C score <sup>a</sup>	Crash score <sup>b</sup>	Polar score <sup>c</sup>	D score <sup>d</sup>	PMF score <sup>e</sup>	G score <sup>f</sup>	Chem score <sup>g</sup>
<b>8k</b>	7.11	-2.14	0.95	-141.56	-6.79	-274.01	-29.59
<b>8l</b>	7.60	-2.04	3.58	-137.31	-12.87	-248.09	-33.75
<b>8m</b>	6.66	-2.05	1.02	-141.94	-10.34	-266.42	-29.10
<b>8n</b>	7.41	-1.30	1.34	-145.63	-11.70	-269.18	-30.69
<b>8o</b>	8.10	-1.77	3.30	-137.75	-6.99	-249.35	-33.00
<b>8p</b>	8.07	-0.90	3.25	-129.32	-37.31	-207.57	-36.22
<b>8q</b>	7.70	-1.58	0.81	-147.40	-8.62	-268.49	-31.63
<b>8r</b>	7.12	-2.50	2.50	-145.62	-6.91	-228.70	-32.89
<b>8s</b>	6.58	-1.42	1.89	-143.49	-23.38	-237.07	-32.10
<b>8t</b>	8.97	-2.99	3.19	-172.77	-18.73	-308.86	-38.23
<b>8u</b>	7.46	-4.95	2.10	-187.92	13.34	-358.21	-39.37
<b>8v</b>	8.60	-1.92	1.85	-148.45	-75.58	-324.49	-35.50
<b>8w</b>	8.68	-0.97	2.44	-144.16	-13.98	-230.02	-31.87
<b>8x</b>	9.98	-2.52	1.88	-161.38	-35.28	-341.01	-41.62
<b>8y</b>	8.09	-1.12	1.02	-139.32	-19.94	-244.81	-30.45
<b>8z</b>	6.98	-2.76	1.60	-143.09	-2.12	-264.18	-30.24

<sup>a</sup>C score (consensus score) integrates a number of popular scoring functions for ranking the affinity of ligands bound to the active site of a receptor and reports the output of total score.

<sup>b</sup>Crash-score revealing the inappropriate penetration into the binding site. Crash scores close to 0 are favorable. Negative numbers indicate penetration.

<sup>c</sup>Polar indicating the contribution of the polar interactions to the total score. The polar score may be useful for excluding docking results that make no hydrogen bonds.

<sup>d</sup>D-score for charge and the van der Waals interactions between the protein and the ligand.

<sup>e</sup>PMF-score indicating the Helmholtz free energies of interactions for protein–ligand atom pairs (Potential of Mean Force, PMF).

<sup>f</sup>G-score showing hydrogen bonding, complex (ligand–protein), and internal (ligand–ligand) energies.

<sup>g</sup>Chem-score points for H-bonding, lipophilic contact, and rotational entropy, along with an intercept term.

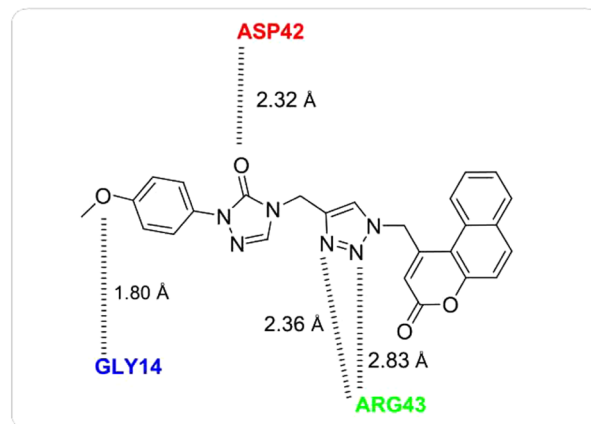
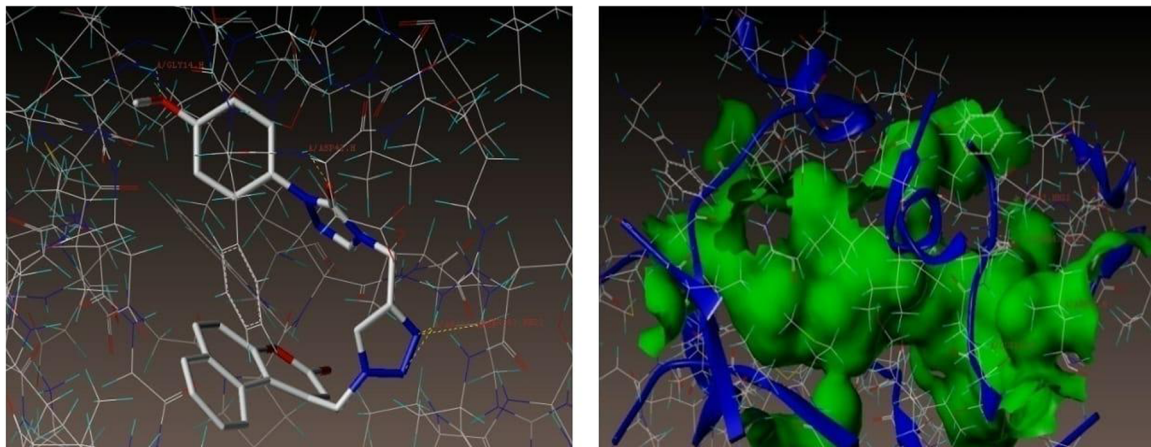


**FIGURE 6** Docked view of compound **8x** at the active site of the enzyme InhA-D148G

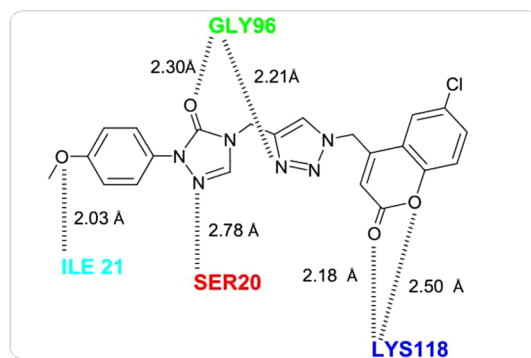
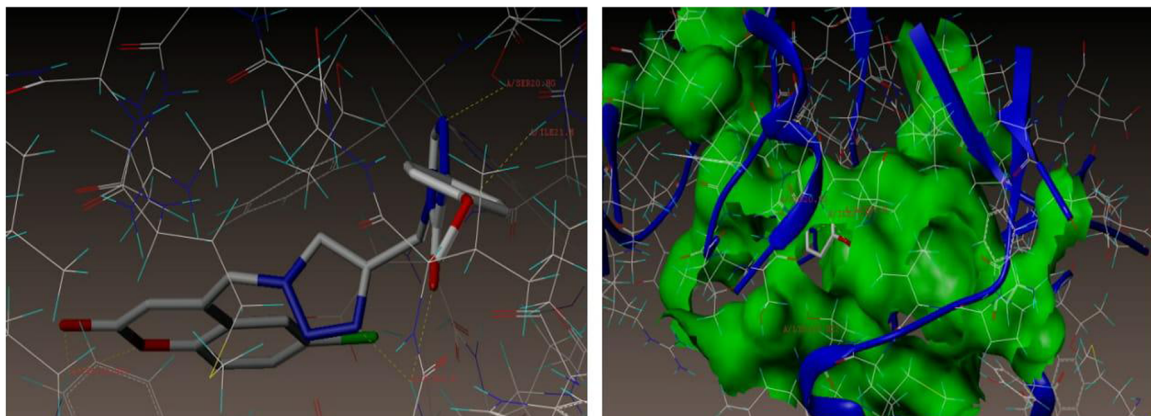


**FIGURE 7** Docked view of compound **8t** at the active site of the enzyme InhA-D148G

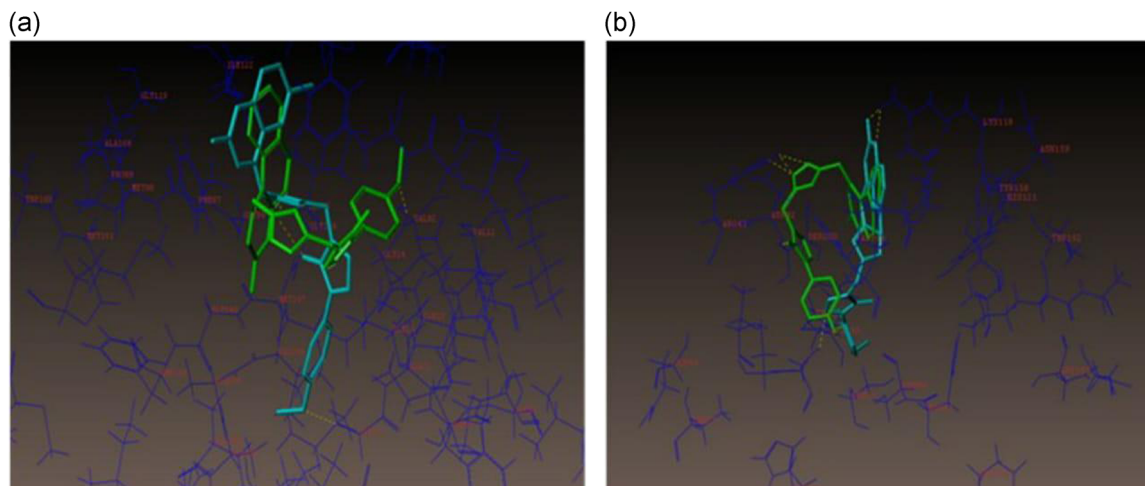


**FIGURE 8** (a) Hydrophobic amino acids surrounding compounds **8x** (green color) and **8t** (cyan color). (b) Hydrophilic amino acids surrounding compounds **8x** and **8t**

2.78 Å), oxygen atom of carbonyl group present on the coumarin ring makes a bonding interaction with hydrogen of LYS118 ( $-C=O-H$ -LYS118, 2.50 Å), oxygen atom present in the coumarin ring makes a bonding interaction with hydrogen of LYS118 ( $-O-H$ -LYS118, 2.18 Å) and oxygen atom of carbonyl group present on the 1,2,4-triazole ring makes a bonding interaction with hydrogen of GLY96 ( $-C=O-H$ -ASP42, 2.21 Å).

Figure 8a,b represents the hydrophobic and hydrophilic amino acids surrounding the compounds **8x** and **8t**.

All docked compounds **8k-z** showed consensus score (C-Score) in the range 9.98–6.58 indicating the summary of all forces of interaction between ligands and the InhA-D148G. Charge and the Van der Waals interactions between protein and ligands varied from  $-129.32$  to  $-187.92$ . The Helmholtz free energies of interactions for protein ligands atom pairs range between  $-2.12$  and  $-75.58$ . However, its H-bonding, complex (ligand-protein), and internal (ligand-ligand) energies range from  $-207.57$  to  $-341.01$ , while those values  $-29.10$  to  $-41.82$  designate the ligands due to H-bonding, lipophilic contact, and rotational entropy, as well as intercept terms (Table 2).

Generally, it was observed that *methoxy* ( $OCH_3$ ) and *carbonyl* ( $C=O$ ) groups and more electronegative atoms present in the molecules form the H-bond with a substrate-binding site of the target enzyme and presence of electron-donating or withdrawing and halogen substitution on the aromatic ring attached to coumarin and 1,2,4-triazole moiety may favor the activity, while those of coumarin, 1,2,3-triazole, 1,2,4-triazole and phenyl moieties help to occupy or penetrate the molecule at the active sites.

### 2.3.3 | *In silico* pharmacokinetics evaluations

We have used Molinspiration<sup>[55]</sup> property calculation program to evaluate whether the synthesized hybrid molecules own the correct pharmacokinetic parameters to exhibit drug-likeness or not. This server predicts molecular descriptors which were used by Lipinski in

formulating the rule of five such as lipophilicity (Log P), molecular weight (MW), number of hydrogen bond donors (donorHB) and acceptors (accptHB), molecular volume (A)3, number of rotatable bonds (NROTB). According to Lipinski, a compound is more likely to be membrane permeable and easily absorbed by the body if it matches the criteria such as (a) MW of compound is less than 500. (b) Its lipophilicity (Log P) is less than 5. (c) The number of groups in the molecule that can accept hydrogen atoms to form hydrogen bonds (HBA) is less than 10. (d) The number of groups in the molecule that can donate hydrogen atoms to hydrogen bonds (HBD) is less than 5. Molinspiration is also used for calculation of Lipinski's violation. In addition, it estimates Topological Polar Surface Area (TPSA; Å<sup>2</sup>). The values of TPSA are used to estimate the percentage of oral absorption (%ABS) by the formula:  $\%ABS = 109 - 0.345TPSA$ .

Theoretical calculation of pharmacokinetic factors (LogP, MW, TPSA, %ABS, number of hydrogen donors and acceptors, NROTB, volume) of all new molecules **8k-z** was carried out and entered in Table 3.<sup>[56,57]</sup> From the data presented in Table 3, it was remarkable that all the described title compounds possess LogP values compatible with those required to cross membranes. TPSA, described to be a predictive indicator of membrane penetration, was also found to be positive. In addition, it can be observed from the table that no violations of Lipinski's rule (MW, LogP, number of hydrogen donors and acceptors) were found, but only one molecule **8u** is in a slight violation regarding (accptHB < 10). This indicates a good predicted oral bioavailability for most of the synthesized molecules.

### 2.3.4 | Toxicity prediction

Toxicity prediction of a newer molecule is an important part of the drug design and development. Computational toxicity findings are not solely faster than the determination of toxic doses in animals, however, they can even facilitate to reduce the number of animal experiments. A web server Protox<sup>[58]</sup> estimates rodent oral toxicity, which is derived from compounds of known drug candidates and



**TABLE 3** *In silico* pharmacokinetics data of the title compounds **8k–z** as predicted by Molinspiration

Code	LogP <sup>a</sup>	M.Wt (<500 amu) <sup>b</sup>	accptHB (<10) <sup>c</sup>	donorHB (<5) <sup>d</sup>	Lipinsk's violation <sup>d</sup>	TPSA <sup>e</sup>	Volumes (A)3 <sup>f</sup>	NROTB <sup>g</sup>	%ABS <sup>h</sup>
<b>8k</b>	2.22	414.43	9	0	0	100.76	355.59	5	74.23
<b>8l</b>	2.45	434.84	9	0	0	100.76	352.57	5	74.23
<b>8m</b>	1.83	430.42	10	0	0	109.99	364.58	6	71.05
<b>8n</b>	3.48	456.51	9	0	0	100.76	405.22	6	74.23
<b>8o</b>	2.22	414.43	9	0	0	100.76	355.59	5	74.23
<b>8p</b>	2.95	450.46	9	0	0	100.76	383.02	5	74.23
<b>8q</b>	2.95	450.46	9	0	0	100.76	383.02	5	74.23
<b>8r</b>	2.60	428.45	9	0	0	100.76	372.15	5	74.23
<b>8s</b>	2.27	444.45	10	0	0	109.99	381.14	6	71.05
<b>8t</b>	2.50	464.87	10	0	0	109.99	378.11	6	71.05
<b>8u</b>	1.88	460.45	11	0	1	119.23	390.1	7	67.86
<b>8v</b>	3.53	486.53	10	0	0	109.99	430.76	7	71.05
<b>8w</b>	2.27	444.45	10	0	0	109.99	381.14	6	71.05
<b>8x</b>	3.01	480.48	10	0	0	109.99	408.57	6	71.05
<b>8y</b>	3.01	480.48	10	0	0	109.99	408.57	6	71.05
<b>8z</b>	2.65	458.48	10	0	0	109.99	397.70	6	71.05

<sup>a</sup>LogP: logarithm of compound partition coefficient between *n*-octanol and water.

<sup>b</sup>M.Wt: molecular weight.

<sup>c</sup>accptHB: number of hydrogen bond acceptors.

<sup>d</sup>donorHB: number of hydrogen bond donors.

<sup>e</sup>TPSA: topological polar surface area.

<sup>f</sup>Volume.

<sup>g</sup>%ABS: percentage of absorption.

<sup>h</sup>NROTB: number of rotatable bonds.

their toxicity by their toxic fragments or chemical structure. The online server Protox compares the similarity of structures of synthesized molecules which will be loaded in a server with info of molecules having antecedently proverbial toxicity and identifies the toxic fragments of loaded molecules and probable toxicity targets. Toxic doses are often known as LD<sub>50</sub> values in mg per kg body weight. The LD<sub>50</sub> is the median lethal dose, meaning the dose at which 50% of test subjects die upon exposure to a compound. The predicted LD<sub>50</sub> (lethal dose) for our target molecules is above 300 mg/kg and less than 1,000 mg/kg for all the tested compounds as shown in Table 4.

The newly synthesized molecules **8k–z** come under the toxicity category of Class IV and there are no toxic fragments present as claimed by the developer's limits. This toxicity prediction study reviews that synthesized molecules can act as the lead molecules for further analysis (Table 4).

### 3 | CONCLUSIONS

The regioselectivity associated with Cu(I) catalyzed azide–alkyne cycloaddition by click reaction under environmentally benign conditions has been confirmed using coumarinyl azides and acetylenic dipolarophile (prepared from sydnone) to get the title compounds **8k–z**. The synthesized compounds were characterized by spectral

analysis and screened for their anti-TB activity. The *in vitro* study of synthesized hybrids **8k–z** yielded some potent entities (*viz.*, **8o**, **8p**, **8s**, **8t**, **8v**, **8w**, and **8x**) owning their potency in micromolar range against *M. tuberculosis* H37Rv (MTB; ATCC-27294) strain. From the cytotoxicity study, we found that compounds **8o**, **8s**, and **8t**, with SI values equal or higher than 153, being more active and less toxic than some drugs used in the treatment of TB. Molecular docking study of all hybrid molecules **8k–z** against InhA as a targeted enzyme for antimycobacterial activity studies was performed to learn binding pattern of the active motifs. Compounds **8t** and **8x** were found to show good binding affinity with the active binding pocket of the InhA enzyme with the highest C score value. The obtained docking results corroborate the experimental findings. Further, the results of pharmacokinetic data and toxicity prediction study provide a confirmation to consider the active molecules as lead targets for further progress in the drug discovery process.

### 4 | EXPERIMENTAL

#### 4.1 | Chemistry

##### 4.1.1 | General

All starting materials and reagents were of analytical grade and were obtained from commercial suppliers and were used without further

**TABLE 4** Toxicity prediction parameters of compounds **8k–z**

Code	Predicted LD <sub>50</sub> (mg/kg)	Predicted toxicity class	Average similarity (%)	Prediction accuracy (%)	Toxic fragments
8k	500	4	42.94	54.26	Nil
8l	500	4	42.82	54.26	Nil
8m	500	4	42.34	54.26	Nil
8n	500	4	43.24	54.26	Nil
8o	500	4	43.13	54.26	Nil
8p	500	4	43.51	54.26	Nil
8q	500	4	43.51	54.26	Nil
8r	500	4	42.57	54.26	Nil
8s	500	4	42.76	54.26	Nil
8t	500	4	42.23	54.26	Nil
8u	500	4	42.40	54.26	Nil
8v	500	4	43.06	54.26	Nil
8w	500	4	42.94	54.26	Nil
8x	500	4	43.30	54.26	Nil
8y	500	4	43.30	54.26	Nil
8z	500	4	42.59	54.26	Nil

Class I: Fatal if swallowed ( $LD_{50} \leq 5$  mg/kg); Class II: Fatal if swallowed ( $5 < LD_{50} \leq 50$  mg/kg); Class III: toxic if swallowed ( $50 < LD_{50} \leq 300$  mg/kg); Class IV: harmful if swallowed ( $300 < LD_{50} \leq 2,000$  mg/kg); Class V: may be harmful if swallowed ( $2,000 < LD_{50} \leq 5,000$  mg/kg); Class VI: nontoxic ( $LD_{50} > 5,000$  mg/kg).

purification (Sigma-Aldrich, S.D. Fine, Alfa Aesar, Spectrochem). All melting points were recorded on Coslab scientific melting point apparatus and are uncorrected. Follow up of the reaction rates by thin-layer chromatography (TLC) was performed on precoated Merck silica gel 60F-254 plates using an appropriate solvent system and the spots were detected under UV lamp ( $\lambda$  254 nm). Infrared spectra (IR) spectra were recorded on a Nicolet 170 SX FT-IR spectrometer, using potassium bromide (KBr) pellets; the frequencies are expressed in  $cm^{-1}$ . Nuclear magnetic resonance ( $^1H$  NMR [400 MHz] and  $^{13}C$  NMR [100 MHz]) spectra were recorded with a Bruker Avance FT NMR spectrometer using tetramethylsilane as the internal reference, with DMSO- $d_6$  as a solvent. The chemical shifts are accounted in parts per million ( $\delta$  ppm). Mass spectra were recorded by using mass spectrometers Shimadzu GCMS-QP2010S and ESI/APCI-Hybrid Quadrupole, Time-of-flight, and LCMS (Synapt G2 HDMS ACQUITY UPLC). Elemental analyses (C, H, and N) were performed on a Heraeus Carlo Erba 1180 CHN analyzer.

Please see the Supporting Information for a complete set of spectral data. The InChI codes of the investigated compounds together with some biological activity data are also provided as Supporting Information.

#### 4.1.2 | Preparation of 2-aryl-4-(prop-2-ynyl)-2H-1,2,4-triazol-3(4H)-ones **4a,b**

To a solution of 2-aryl-2H-1,2,4-triazol-3(4H)-ones **3a,b** (0.02 M) in dry acetone, anhydrous  $K_2CO_3$  (0.02 M), and 3-bromoprop-1-yne (0.02 M) were added. The reaction mixture was stirred at RT for 4 hr. The completion of the reaction was observed by TLC using a mixture

of ethyl acetate and hexane (2:8) as an eluent. After completion of the reaction the solvent was removed under reduced pressure and after evaporation colourless crystals of compounds **4a,b**.<sup>[59,60]</sup>

#### 4.1.3 | Preparation of 4-bromomethyl-coumarins **6c–j**

Substituted-4-bromomethyl coumarins have been prepared via Pechmann cyclization of substituted phenols **5c–j** with ethyl-4-bromoacetoacetate.<sup>[61,62]</sup>

#### 4.1.4 | Preparation of 4-(azidomethyl)-2H-chromen-2-ones **7c–j**

4-Bromomethyl coumarins **6c–j** (0.010 M) were taken in acetone (20 ml) in a round-bottom flask. To this, sodium azide (0.012 M) in water (3 ml) was added drop wise with stirring, which was continued for 10 hr. The reaction blend was then poured into ice-cold water. Separated solid was filtered and recrystallized using ethanol to afford **7c–j**.<sup>[63,64]</sup>

#### 4.1.5 | Synthesis of coumarin-3-yl-methyl-1,2,3-triazolyl-1,2,4-triazol-3(4H)-ones **8k–z**

To a solution of 2-aryl-4-(prop-2-ynyl)-2H-1,2,4-triazol-3(4H)-ones **4a,b** (1.00 M) in THF/ $H_2O$ , 1:1(v/v),  $CuSO_4 \cdot 5H_2O$  (0.15 M) and sodium ascorbate (0.30 M) were added. The mixture was stirred at room temperature for 15 min and 7-methyl-4-azidomethyl coumarins **7c–j** (1.00 M) were added. The resulting reaction mixture was

continued to stir until the starting material was consumed (TLC). The reaction mixture was then cooled, separated solid was filtered and washed with water and recrystallised from ethyl acetate to get the crystals of desired products **8k–z**.

4-((1-((6-Methyl-2-oxo-2H-chromen-4-yl)methyl)-1H-1,2,3-triazol-4-yl)methyl)-2-phenyl-2H-1,2,4-triazol-3(4H)-one (**8k**)

Greenish yellow (yield: 95%); Mp: 102–104°C; IR (KBr,  $\text{cm}^{-1}$ ): 1723 (coumarin, C=O), 1698 (1,2,4-triazolin, C=O), 1629 (C=N);  $^1\text{H}$  NMR (400 MHz, DMSO- $d_6$ )  $\delta$  (ppm): 2.34 (s, 3H,  $-\text{CH}_3$ ), 4.96 (s, 2H, coumain  $\text{C}_4-\text{CH}_2$ ), 5.80 (s, 2H, 1,2,4-triazolin  $\text{N}_4-\text{CH}_2$ ), 5.95 (s, 1H,  $\text{H}_3$  coumain pyran ring), 6.96–7.70 (m, 8H, Ar-H), 8.24 (s, 1H, 1,2,3-triazole  $\text{C}_5\text{H}$ ), 8.30 (s, 1H, 1,2,4-triazolin  $\text{C}_5\text{H}$ );  $^{13}\text{C}$  NMR (100 MHz, DMSO- $d_6$ )  $\delta$  (ppm): 20.32, 37.11, 48.99, 113.65, 114.09, 116.43, 119.78, 124.32, 124.80, 130.67, 133.25, 133.76, 137.45, 142.43, 149.33, 150.64, 151.19, 156.32, 159.38; MS,  $m/z$  (70 eV): 414 [ $\text{M}^+$ ]; CHN analysis for  $\text{C}_{22}\text{H}_{18}\text{N}_3\text{O}_6$  (%): Calcd: C 63.76, H 4.38, N 20.28 Found: C 63.81, H 4.40, N 20.32.

## 4.2 | Biological activity

### 4.2.1 | Antitubercular activity assay

The antitubercular activity of the compounds **8k–z** was assessed against *M. tuberculosis* using MABA. This methodology is nontoxic, employs a thermally stable reagent, and shows good correlation with proportional and BACTEC radiometric method. Sterile de-ionized water (200  $\mu\text{l}$ ) was added to all outer perimeter wells of sterile 96 wells plate to minimize the evaporation of medium in the test wells during incubation. The 96-well plate received 100  $\mu\text{l}$  of the Middle Brook 7H9 broth and serial dilution of compounds was made directly on the plate. The final drug concentrations tested were 100 to 0.20  $\mu\text{g}/\text{ml}$ . Plates were enclosed and preserved with parafilm and incubated at 37°C for 5 days. After this freshly prepared 1:1 mixture of Almar Blue reagent (25  $\mu\text{l}$ ) and 10% Tween 80 was added to the plate and incubated for 24 hr. Blue color in the well was understood as no bacterial growth, and pink color was scored as growth. The MIC was defined as the lowest drug concentration which prevented the color change from blue to pink.<sup>[64]</sup>

### 4.2.2 | Cytotoxicity evaluation

#### Cell culture

This is a colorimetric assay that measures the reduction of yellow 3-(4,5-dimethylthiazol-2-yl)-2,5-diphenyl tetrazolium bromide (MTT) by mitochondrial succinate dehydrogenase. The MTT enters the cells and passes into the mitochondria where it is reduced to an insoluble, colored (dark purple) formazan product. The cells are then solubilized with an organic solvent (e.g., DMSO, isopropanol) and the released, solubilized formazan reagent is measured spectrophotometrically. Since the reduction of MTT can only occur in metabolically active cells the level of activity is a measure of the viability of the cells.<sup>[65]</sup>

Cell line: HEK293 (human embryonic kidney); media: DMEM with low glucose (Cat No.-11965-092); materials: FBS (Gibco, Invitrogen)

Cat. No. 10270106, Antibiotic – Antimycotic 100 $\times$  solution (Thermo Fisher Scientific) Cat. No. 15240062, 96-well plates.

#### Cytotoxicity assay

The cells were seeded at a density of approximately  $5 \times 10^3$  cells/well in a 96-well flat-bottom microplate and maintained at 37°C in 95% humidity and 5%  $\text{CO}_2$  for overnight. Different concentrations (600, 300, 150, 75, 37.5, and 18.75  $\mu\text{M}$ ) of samples was treated. The cells were incubated for another 48 hr. The cells in well were washed twice with phosphate buffer solution, and 20  $\mu\text{l}$  of the MTT staining solution (5 mg/ml in phosphate buffer solution) was added to each well and plate was incubated at 37°C. After 4 hr, 100  $\mu\text{l}$  of dimethyl sulfoxide (DMSO) was added to each well to dissolve the formazan crystals, and absorbance was recorded with a 570 nm using microplate reader (1, 2).

Surviving cells (%) = Mean OD of test compound / Mean OD of negative control  $\times$  100.

Using GraphPad Prism Version 5.1, we calculated the  $\text{IC}_{50}$  of compounds.

Note: DMSO concentration is less 1.5% in experiments and concentrations are in duplicates.

## 4.3 | Molecular docking studies

Molecular modeling was carried out using Sybyl-X, version 2.0,<sup>[66]</sup> running on a Intel® Core™ i3-2130 CPU@3.40 GHz processor using Windows 7 professional workstation. Surflex-Dock algorithm of Sybyl-X 2.0 was used to dock designed compounds. The crystal structure of *M. tuberculosis* InhA-D148G mutant in complex with NADH was downloaded from the Protein Data Bank (PDB entry code 4DQU extracted from the Brookhaven Protein Database <http://www.rcsb.org/pdb>) and used for initial docking studies. Co-crystallized ligand was removed from the structure, water molecules were removed, essential H atoms were added and side chains were fixed during protein preparation. The structure was then subjected to an energy refinement procedure. Gasteiger-Huckel charges<sup>[67]</sup> were calculated for the ligand, while Amber 7FF02 was used for the protein. The model was then subjected to energy minimization following the gradient termination of the Powell method for 3000 iterations using the Tripos force field with nonbonding cut offset at 9.0 and the dielectric constant set at 4.0. The binding of the substituted coumarin derivatives was also estimated using a variety of scoring functions that have been compiled into the single consensus score (C Score).

## ACKNOWLEDGMENTS

The authors are thankful to the University Grants Commission (UGC), New Delhi (F. No. 14-3/2012 [NS/PE] Dated: 14-03-2012) for providing infrastructural and chemical facilities under “Antitumor Activity an Integrated Approach” a focused area of UPE FAR-I program. We articulate our appreciation to the USIC, K. U. Dharwad, NMR Research Centre, IISc Bengaluru and Institution of Excellence,

Mysore University, India for carrying out the spectral analyses. We forward our gratefulness to UGC, New Delhi for providing financial aid to one of the author S. M. S. in the form of project fellowship under UPE FAR- I program.

## CONFLICT OF INTERESTS

The authors declare that there is no conflict of interest.

## ORCID

Ravindra R. Kamble  <http://orcid.org/0000-0002-0384-655X>

## REFERENCES

- J. P. Cegielski, D. P. Chin, M. A. Espinal, T. R. Frieden, R. R. Cruz, E. A. Talbot, D. E. C. Weil, R. Zaleskis, M. C. Raviglione, *Infect. Dis. Clin. North Am.* **2002**, *161*, 1.
- M. K. Spigelman, *J. Infect. Dis.* **2007**, *196*, S28.
- J. C. Sacchettini, E. J. Rubin, J. S. Freundlich, *Nat. Rev. Microbiol.* **2008**, *6*, 41.
- D. J. Payne, M. N. Gwynn, D. J. Holmes, D. L. Pompliano, *Nat. Rev. Drug Discov.* **2007**, *6*, 29.
- M. Whiting, J. Muldoon, Y. C. Lin, S. M. Silverman, W. Lindstrom, A. J. Olson, H. C. Kolb, M. G. Finn, K. B. Sharpless, J. H. Elder, V. V. Fokin, *Angew. Chem. Int. Ed. Engl.* **2006**, *45*, 1435.
- C. W. Tornøe, S. J. Sanderson, J. C. Mottram, G. H. Coombs, M. Meldal, *J. Comb. Chem.* **2004**, *6*, 312.
- I. S. Bennett, G. Brooks, N. J. P. Broom, S. H. Calvert, K. Coleman, I. François, *J. Antibiot.* **1991**, *44*, 969.
- M. S. Costa, N. Boechat, É. A. Rangel, F. C. Da Silva, A. M. T. De Souza, C. R. Rodrigues, H. C. Castro, I. N. Junior, M. C. S. Lourenço, S. M. S. V. Wardell, V. F. Ferreira, *Bioorg. Med. Chem.* **2006**, *14*, 8644.
- C. Gill, G. Jadhav, M. Shaikh, R. Kale, A. Ghawalkar, D. Nagargoje, M. Shiradkar, *Bioorg. Med. Chem. Lett.* **2008**, *18*, 6244.
- B. K. Singh, A. K. Yadav, B. Kumar, A. Gaikwad, S. K. Sinha, V. Chaturvedi, R. P. Tripathi, *Carbohydr. Res.* **2008**, *343*, 1153.
- H. Gallardo, G. Conte, F. Bryk, M. C. S. Lourenço, M. S. Costa, V. F. Ferreira, *J. Braz. Chem. Soc.* **2007**, *18*, 1285.
- H. Wamhoff, in *Comprehensive Heterocyclic Chemistry* (Eds: A. R. Katritzky, C. W. Rees), Pergamon, Oxford **1984**, vol. 5, pp. 669-732.
- H. C. Kolb, M. G. Finn, K. B. Sharpless, *Angew. Chem. Int. Ed. Engl.* **2001**, *40*, 2004.
- C. W. Tornøe, C. Christensen, M. Meldal, *J. Org. Chem.* **2002**, *67*, 3057.
- V. V. Rostovtsev, L. G. Green, V. V. Fokin, K. B. Sharpless, *Angew. Chem. Int. Ed. Engl.* **2002**, *41*, 2596.
- D. Baraniak, K. Kacprzak, L. Celewicz, *Bioorg. Med. Chem. Lett.* **2011**, *21*, 723.
- S. Punna, D. D. Diaz, C. Li, K. B. Sharpless, V. V. Fokin, M. G. Finn, *Am. Chem. Soc., Div. Polym. Chem.* **2004**, *45*, 778.
- L. V. Lee, M. L. Mitchell, S. J. Huang, V. V. Fokin, K. B. Sharpless, C. H. Wong, *J. Am. Chem. Soc.* **2003**, *125*, 9588.
- T. S. Seo, Z. Li, H. Ruparel, J. Ju, *J. Org. Chem.* **2003**, *68*, 609.
- Q. Wang, T. R. Chan, R. Hilgraf, V. V. Fokin, K. B. Sharpless, M. G. Finn, *J. Am. Chem. Soc.* **2003**, *125*, 3192.
- S. Löber, P. Rodriguez-Loaiza, P. Gmeiner, *Org. Lett.* **2003**, *5*, 1753.
- F. Pérez-Balderas, M. Ortega-Muñoz, J. Morales-Sanfrutos, F. Hernández-Mateo, F. G. Calvo-Flores, J. A. Calvo-Asín, J. Isac-García, F. Santoyo-González, *Org. Lett.* **2003**, *5*, 1951.
- M. Iranshahi, M. Askari, A. Sahebkar, D. Adjipavlou-Litina, *DARU J. Pharm. Sci.* **2009**, *17*, 99.
- A. Thakur, R. Singla, V. Jaitak, *Eur. J. Med. Chem.* **2015**, *101*, 476.
- S. Rosselli, A. M. Maggio, N. Faraone, V. Spadaro, S. L. Morris-Natschke, K. F. Bastow, K. H. Lee, M. Bruno, *Nat. Prod. Commun.* **2009**, *4*, 1701.
- C. M. Teng, C. H. Lin, F. N. Ko, T. S. Wu, T. F. Huang, *Schmiedebergs Arch. Pharmacol.* **1994**, *349*, 202.
- S. K. Poole, C. F. Poole, *Analyst* **1994**, *119*, 113.
- E. G. Crichton, P. G. Waterman, *Phytochemistry* **1978**, *17*, 1783.
- A. D. Patil, A. J. Freyer, D. S. Eggleston, R. C. Haltiwanger, M. F. Bean, P. B. Taylor, M. J. Caranfa, A. L. Breen, H. R. Bartus, *J. Med. Chem.* **1993**, *36*, 4131.
- C. Spino, M. Dodier, S. Sotheeswaran, *Bioorg. Med. Chem. Lett.* **1998**, *8*, 3475.
- W. K. Whang, H. S. Park, I. Ham, M. Oh, H. Namkoong, H. K. Kim, D. W. Hwang, S. Y. Hur, T. E. Kim, Y. G. Park, J. R. Kim, J. W. Kim, *Exp. Mol. Med.* **2005**, *37*, 436.
- N. K. Swarnakar, A. K. Jain, R. P. Singh, C. Godugu, M. Das, S. Jain, *Biomaterials* **2011**, *32*, 6860.
- E. Shin, K. M. Choi, H. S. Yoo, C. K. Lee, B. Y. Hwang, M. K. Lee, *Biol. Pharm. Bull.* **2010**, *33*, 1610.
- N. I. Baek, E. M. Ahn, H. Y. Kim, Y. D. Park, *Arch. Pharm. Res.* **2000**, *23*, 467.
- D. M. Fort, K. Rao, S. D. Jolad, J. Luo, T. J. Carlson, S. R. King, *Phytomedicine* **2000**, *6*, 465.
- K. Luo, J. Sun, J. Y. W. Chan, L. Yang, S. Wu, K. P. Fung, F. Liu, *Chemotherapy* **2011**, *57*, 449.
- N. Piller, *Br. J. Exp. Pathol.* **1975**, *56*, 554.
- R. J. Naik, M. V. Kulkarni, K. Sreedhara Ranganath Pai, P. G. Nayak, *Chem. Biol. Drug Des.* **2012**, *80*, 516.
- M. R. Shiradkar, K. K. Murahari, H. R. Gangadasu, T. Suresh, C. A. Kalyan, D. Panchal, R. Kaur, P. Burange, J. Ghogare, V. Mokale, M. Raut, *Bioorg. Med. Chem.* **2007**, *15*, 3997.
- G. R. Thompson, J. Cadena, T. F. Patterson, *Clin. Chest Med.* **2009**, *30*, 203.
- D. Zampieri, M. G. Mamolo, E. Laurini, G. Scialino, E. Banfi, L. Vio, *Arch. Pharm. Chem. Life Sci.* **2009**, *342*, 716.
- N. B. Patel, I. H. Khan, S. D. Rajani, *Arch. Pharm. Chem. Life Sci.* **2010**, *10*, 692.
- S. M. Somagond, R. R. Kamble, P. P. Kattimani, S. K. J. Shaikh, S. R. Dixit, S. D. Joshi, H. C. Devarajogwda, *ChemistrySelect* **2018**, *3*, 2004.
- Z. Li, Y. Liu, X. Bai, Q. Deng, J. Wang, G. Zhang, C. Xiao, Y. Mei, Y. Wang, *RSC Adv.* **2015**, *5*, 97089.
- Z. Li, X. Bai, Q. Deng, G. Zhang, L. Zhou, Y. Liu, J. Wang, Y. Wang, *Bioorg. Med. Chem.* **2017**, *25*, 213.
- A. Anand, R. J. Naik, H. M. Revankar, M. V. Kulkarni, S. R. Dixit, S. D. Joshi, *Eur. J. Med. Chem.* **2015**, *105*, 194.
- M. Basanagouda, V. B. Jambagi, N. N. Barigidad, S. S. Laxmeshwar, V. Devaru, Narayanachar, *Eur. J. Med. Chem.* **2014**, *74*, 225.
- M. U. Rahman, A. Rathore, A. A. Siddiqui, G. Parveen, M. Shahar Yar, *J. Enzyme Inhib. Med. Chem.* **2014**, *29*, 733.
- A. Müller-Schiffmann, H. Sticht, C. Korth, *Bio Drugs* **2012**, *26*, 21.
- A. Husain, M. Rashid, R. Mishra, S. Parveen, D. S. Shin, D. Kumar, *Bioorg. Med. Chem. Lett.* **2012**, *22*, 5438.
- M. Asif, A. Kaur, *J. Pharma. Toxicol.* **2015**, *1*, 6.
- F. R. Pavan, P. I. da S. Maia, S. R. A. Leite, V. M. Deflon, A. A. Batista, D. N. Sato, S. G. Franzblau, C. Q. F. Leite, *Eur. J. Med. Chem.* **2010**, *45*, 1898.
- I. Orme, J. Secrist, S. Anathan, C. Kwong, J. Maddry, R. Reynolds, A. Poffenberger, M. Michael, L. Miller, J. Krahenbuh, L. Adams, A. Biswas, S. Franzblau, D. Rouse, D. Winfield, J. Brooks, *Antimicrob. Agents Chemother.* **2001**, *45*, 1943.
- L. A. Collins, S. G. Franzblau, *Antimicrob. Agents Chemother.* **1997**, *41*, 1004.

- [55] Molinspiration Cheminformatics, <http://www.molinspiration.com/cgi-bin/properties>.
- [56] C. A. Lipinski, F. Lombardo, B. W. Dominy, P. J. Feeney, *Adv. Drug Deliv. Rev.* **1997**, 23, 3.
- [57] P. Ertl, B. Rohde, P. Selzer, *J. Med. Chem.* **2000**, 43, 3714.
- [58] S. K. Dutta, S. K. Basu, K. K. Sen, *J. Expt. Biol.* **2006**, 44, 123.
- [59] T. Batool, N. Rasool, Y. Gull, M. Noreen, N. Faiz-ul-Hassan, A. Yaqoob, M. Zubair, U. A. Rana, S. Ud-Din Khan, M. Zia-UI-Haq, H. Z. E. Jaafar, *PLoS One* **2014**, 9, e115457.
- [60] M. Basanagouda, M. V. Kulkarni, *Synth. Commun.* **2011**, 41, 2569.
- [61] A. Burger, G. E. Ullyot, *J. Org. Chem.* **1947**, 12, 342.
- [62] R. A. Kusanur, M. V. Kulkarni, G. M. Kulkarni, S. K. Nayak, T. N. Guru Row, K. Ganesan, C. M. Sun, *J. Heterocycl. Chem.* **2010**, 47, 91.
- [63] R. J. Naik, M. V. Kulkarni, *J. Lumin.* **2010**, 130, 2065.
- [64] M. C. Lourenco, M. V. N. De'Souza, A. C. Pinheiro, M. L. Ferreira, R. B. Goncalves, T. C. M. Nogueira, M. A. Peralta, *ARKIVOC* **2007**, 15, 181.
- [65] M. R. Peram, S. S. Jalalpure, V. M. Kumbar, S. R. Patil, S. A. Joshi, K. G. Bhat, P. V. Diwan, *J. Liposome Res.* **2018**, 7, 1.
- [66] Tripos International, Sybyl-X 2.0, Tripos International. St. Louis, MO, **2012**.
- [67] J. Gasteiger, M. Marsili, *Tetrahedron* **1980**, 36, 3219.

**How to cite this article:** Somagond SM, Kamble RR, Bayannavar PK, et al. Click chemistry based regioselective one-pot synthesis of coumarin-3-yl-methyl-1,2,3-triazolyl-1,2,4-triazol-3(4H)-ones as newer potent antitubercular agents. *Arch Pharm Chem Life Sci.* 2019;e1900013. <https://doi.org/10.1002/ardp.201900013>